(c)2001 American Institute of Aeronautics & Astronautics or Published with Permission of Author(s) and/or Author(s)' Sponsoring Organization.

15th AIAA Computational Fluid Dynamics Conference
11-14 June 2001 Anaheim, CA

A01-31074

AIAA 2001-2581

MULTIOBJECTIVE OPTIMIZATION OF ROCKET ENGINE PUMPS USING EVOLUTIONARY ALGORITHM

Akira Oyama*
NASA Glenn Research Center
Ohio Aerospace Institute, 22800 Cedar Point Rd., Cleveland, OH 44142, USA
(440) 962-3148, aoyama@dino.grc.nasa.gov
and
Meng-Sing Liou†
NASA Glenn Research Center, MS 5-11, Cleveland, OH 44135, USA
(216) 433-5855, meng-sing.liou@grc.nasa.gov

ABSTRACT

Design optimization method for turbopumps of cryogenic rocket engines has been developed. Multiobjective Evolutionary Algorithm is used for multiobjective pump design optimizations. Performances of design candidates are evaluated by using the meanline pump flow modeling method based on the Euler turbine equation coupled with empirical correlations for rotor efficiency.

To demonstrate the feasibility of the present approach, single stage centrifugal pump design and multistage pump design optimizations are presented. In both cases, present method obtains very reasonable Pareto-optimal solutions that include some designs outperforming the original design in total head as well as input power by 1%. Detailed observation of the design results also reveals some important design policies in turbopump design of cryogenic rocket engines. These results ensure the feasibility of EA-based design optimization method in this field.

INTRODUCTION

While budget for space development programs has drastically shrunk in most countries, recent and future space missions increasingly demand high performance and reliability for rocket engine systems and their components, such as turbopumps. Though the progress in computational fluid dynamics (CFD) methods and development of powerful computational facilities have contributed to reduce necessary cost and time required to develop the advanced turbopump designs, the design process still largely depends on experienced designers. Therefore, numerical design methods coupled with CFD capable of efficiently developing advanced turbopump designs can greatly reduce such dependency.

Among numerical optimization algorithms, gradient-based methods are long-standing and most widely used approaches[1-3]. These methods use gradient of an objective function with respect to changes in design variables to calculate a search direction using steepest descent, conjugate gradient, quasi Newton techniques, or adjoint formulations. The solution obtained by these methods will be a global optimum, only if the objective and constraints are differentiable and convex[4]. Unfortunately, distribution of an objective function of real-world design problems is usually multimodal and one could only hope for a local optimum neighboring the initial design point. Therefore, to determine the global optimum, one must optimize from a number of initial points and check for consistency in the optima obtained. In this sense, the gradient-based methods are not robust.

Evolutionary Algorithms (EAs, for example, see [5]) are emergent design optimization algorithms modeled on mechanism of the natural evolution. EAs search from multiple points, instead of moving from a single

* NRC Research Associate, Member AIAA
† Senior Scientist, Associate Fellow AIAA

Copyright © 2001 by the American Institute of Aeronautics and Astronautics, Inc. No copyright is asserted in the United States under Title 17, U.S. Code. The U.S. Government has a royalty-free license to exercise all rights under the copyright claimed herein for Governmental purposes. All other rights are reserved by the copyright owner.

(c)2001 American Institute of Aeronautics & Astronautics or Published with Permission of Author(s) and/or Author(s)' Sponsoring Organization.

point. In addition, they require no derivatives or gradients of the objective function. These features lead to robustness and simplicity in coupling any evaluation codes. Parallel efficiency also becomes very high by using a simple master-slave concept for function evaluations, if such evaluations consume most of CPU time. Design optimization using CFD is a typical case. Application of EAs to multiobjective design problems is also straightforward because EAs maintain a population of design candidates in parallel. Due to these advantages, EAs are unique and attractive approach to real-world design optimization problems. Recently, EAs have been successfully applied to aerospace design optimization problems[5-9].

The objective of the present study is to develop and demonstrate a design optimization method for turbopumps of cryogenic rocket engines. Multiobjective Evolutionary Algorithm (MOEA) will be used for multiobjective optimization of pump designs. Performances of design candidates will be evaluated by using the meanline pump flow modeling method based on the Euler turbine equation coupled with empirical correlations for rotor efficiency. Present approach will be applied to centrifugal and multistage turbopump design optimization problems.

EVOLUTIONARY ALGORITHMS

EAs mimic mechanism of natural evolution, where a biological population evolves over generations to adapt to an environment by selection according to fitness, recombination and mutation of genes (Fig.1). When EAs are applied to optimization problems, individual, fitness, and genes usually correspond to a design candidate, an objective function value, and design variables, respectively. One of the key features of EAs is that they search from multiple points in the design space, instead of moving from a single point like gradient-based methods do. Furthermore, these methods work on function evaluations alone and do not require derivatives or gradients of the objective

Pareto-optimal solutions. Each of those solutions is optimal in the sense that no improvement can be achieved in one objective component that does not lead to degradation in at least one of the remaining components. Therefore, primary goal of a multiobjective optimization problem is, unlike that of a single objective optimization, to find various Pareto-optimal solutions to show the precise tradeoff information among the completing objectives. By maintaining a population of solutions and introducing the concept of Pareto-optimality, EAs can uniformly sample various Pareto-optimal solutions in parallel.

3) Suitability to parallel computing: Since EAs are population-based search algorithms, all design candidates in each generation can be evaluated in parallel by using the simple master-slave concept. Parallel efficiency is also very high, if objective function evaluations consume most of CPU time.
4) Simplicity in coupling evaluation codes: As these methods use only objective function values of design candidates, EAs do not need substantial modification or sophisticated interface to evaluation codes. If an all-out re-coding were required to every optimization problem like the adjoint methods, extensive validation of the new code would be necessary every time. EAs can save such troubles.

The present MOEA uses floating-point representation. Fonseca's Pareto-based ranking method is used for fitness assignment where an individual's rank corresponds to the number of individuals in the current population that are better than the corresponding individual in every objective function. To maintain diversity in the population, a standard sharing function[10] is incorporated. As the elitism, the best-N selection[11] is incorporated, where the best N individuals are selected for the next generation among N parents and N children based on Pareto-optimality[5] so that Pareto-optimal solutions will be kept once they

(c)2001 American Institute of Aeronautics & Astronautics or Published with Permission of Author(s) and/or Author(s)' Sponsoring Organization.

meanline pump flow modeling method, which provides a fast capability for modeling turbopumps within rocket engines. The components of the inlet and exit fluid velocity triangles are calculated at the hub, mean and tip locations along the rotor blades. The meridional velocity of the fluid at the rotor leading edge root

mean-square diameter C_{M1} [ft/sec] is defined by equation (1).

$$C_{M1} = \frac{144m}{\rho_1 A_1} \tag{1}$$

where

m: Mass flow [lbs/sec]

ρ_1: Fluid density at leading edge [lbs/ft^3]

A_1: Flow area at leading edge [inch^2]

Flow area is calculated from the input flow path dimensions.

$$A = \lambda\left[\pi B\left(R_{hub} + R_{tip}\right) - block\right] \tag{2}$$

where

λ: Boundary layer blockage factor

B: Blade span from hub to tip [inch]

R_{hub}: Radial distance from pump centerline at hub [inch]

R_{tip}: Radial distance from pump centerline at tip [inch]

The metal blockage of the rotor *block* is calculated by eq. (3).

$$block = \frac{thk \cdot B \cdot Z}{\sin\beta} \tag{3}$$

where

thk: Normal blade thickness [inch]

Z: Blade number

β: Relative angle from tangential [degree]

The tangential component of velocity entering the rotor is calculated in terms of the swirl angle of the flow α_1 by equation (4).

$$C_{U1} = C_{M1} / \tan(\alpha_1) \tag{4}$$

of the fluid relative velocity W_{U2} are given by equations (7) and (8), respectively.

$$U = \frac{2\pi \cdot R \cdot N}{720} \tag{7}$$

$$W_{U2} = C_{M2} \cdot \tan\beta_2 + U_2(1-\sigma) \tag{8}$$

where

R: Radial distance from pump centerline [inch]

N: Shaft rotative speed [rpm]

β_2: Relative angle from tangential at trailing edge [degree]

The slip factor σ is defined by

$$\sigma = 1 - \frac{slip}{U_2} \tag{9}$$

The slip is the difference between the theoretical and absolute fluid tangential velocities. For centrifugal impellers, Pfleiderer correlation to geometry[13] is used to calculate the slip factor σ. A default slip factor of 0.95 is used for inducers.

The head rise through the rotor is calculated iteratively from the Euler turbine equation coupled with empirical correlations for rotor efficiency

$$H_2 = \frac{\left(U_2 \cdot C_{U2} - U_1 \cdot C_{U1}\right)}{g_c} \cdot \eta_{hyd} \tag{10}$$

where

H_2: Head rise through the rotor [ft]

η_{hyd}: Rotor hydraulic efficiency

g_c: Gravitational constant, 32.174[lbm-ft/lbf-sec^2]

The rotor hydraulic efficiency is obtained from empirical correlations to rotor-specific speed[14]. The total pressure and static pressure at the rotor exit are estimated from the rotor head rise by equations (11) and (12).

$$P_{t2} = \frac{H_2 \cdot \rho_{1-2}}{144} + P_{t1} \tag{11}$$

(c)2001 American Institute of Aeronautics & Astronautics or Published with Permission of Author(s) and/or Author(s)' Sponsoring Organization.

where design point total pressure loss coefficient of the diffusion system is assumed to be known and is input in terms of a normalized loss coefficient $\omega_{2\text{-}4}$. The total head rise through pump is calculated by

$$H_4 = \frac{144 \cdot (P_{t4} - P_{t1})}{\rho_{1-4}} \tag{15}$$

where

H_4: Total head rise through pump [ft]

η_{mech}: Mechanical efficiency

η_{vol} : Volumetric efficiency

PL_{disk}: Disk Pumping loss [hp]

The mechanical efficiency is assumed to be 0.98 and the volumetric efficiency is based on internal leakages and is expressed as the ratio of leakage to the inlet flow. The disk pumping loss is calculated from empirical correlations to geometry, fluid density at

(c)2001 American Institute of Aeronautics & Astronautics or Published with Permission of Author(s) and/or Author(s)' Sponsoring Organization.

blade thickness (*thk*), blade trailing edge angle at the hub, root-mean-square radius, and tip (β_{hub} , β_{mid} , β_{tip}) as shown in Fig. 2. Table 1 presents present design spaces.

Total head and input power of Pareto-optimal designs, original design, and all other design candidates are illustrated in Fig. 3. Designs that have cavitation are eliminated from the figure. Present Pareto-optimal solutions successfully displays tradeoff information between maximization of the total head and minimization of the input power. Such tradeoff information is very helpful to a higher-level decision-maker in selecting a design with other considerations. Among the Pareto-optimal solutions, some designs outperform the original design in the total head as well as the input power by 1%.

Figure 4 compares overall performance maps of the original design, the highest total head design, the lowest input power design, and a compromised design that overcomes the original design in both objectives. The compromised design improved the exit pressure in all off-design conditions. The design parameters of these designs are shown in Table 2.

The absolute flow velocity at rotor exit hub is show in Fig. 5. This figure indicates the optimum designs have small exit flow velocity, which contributes to minimize

consisting of one inducer and a single centrifugal impeller, followed by a vaneless diffuser and conical exit volute. The objectives are maximization of total head and minimization of input power at the design point, which is shaft rotative speed of 12,900[rpm], total temperature of the fluid entering the pump of 175 [Rankin], total pressure of the fluid entering the pump of 40.0 [psia], and mass flow into the pump of 40.0 [lbm/sec]. Design parameters and the corresponding parameter ranges are shown in Fig. 7 and Table 3, respectively.

Figure 8 shows total head and input power of Pareto-optimal designs, original design, and all other design candidates that have no cavitation. Though this design optimization problem involves two stages and a large number of design parameters, present MOEA finds reasonable Pareto-optimal solutions including some designs that improve both total head and input power by as much as 1%.

Figure 9 shows overall performance maps of the original design and optimized designs. The compromised design improved the exit pressure in all off-design conditions. The design parameters of these designs are shown in Table 4.

Figures 10 and 11 illustrate the head rise and the required input power of the first and the second stages

(c)2001 American Institute of Aeronautics & Astronautics or Published with Permission of Author(s) and/or Author(s)' Sponsoring Organization.

SUMMARY

In the present study, a design optimization method for turbopumps of cryogenic rocket engines has been developed. Multiobjective Evolutionary Algorithm is used for the multiobjective optimization of pump

Algorithms Coupled with CFD solver," European Congress on Computational Methods in Applied Sciences and Engineering, Barcelona, Spain, September 2000.

[9] Sasaki, D., Obayashi, S., Sawada, K. and Himeno,

(c)2001 American Institute of Aeronautics & Astronautics or Published with Permission of Author(s) and/or Author(s)' Sponsoring Organization.

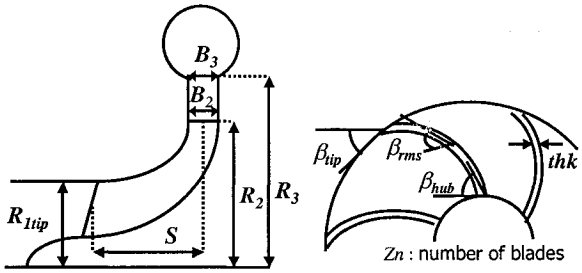

Figure 2. Design parameters of the centrifugal pump design problem.

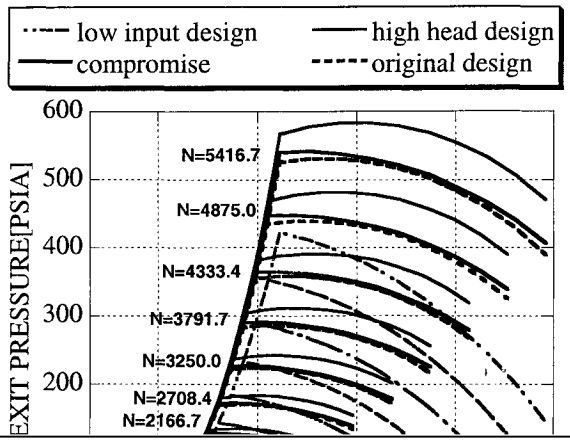

Table 1. Design parameter ranges of the centrifugal pump design problem.

(c)2001 American Institute of Aeronautics & Astronautics or Published with Permission of Author(s) and/or Author(s)' Sponsoring Organization.

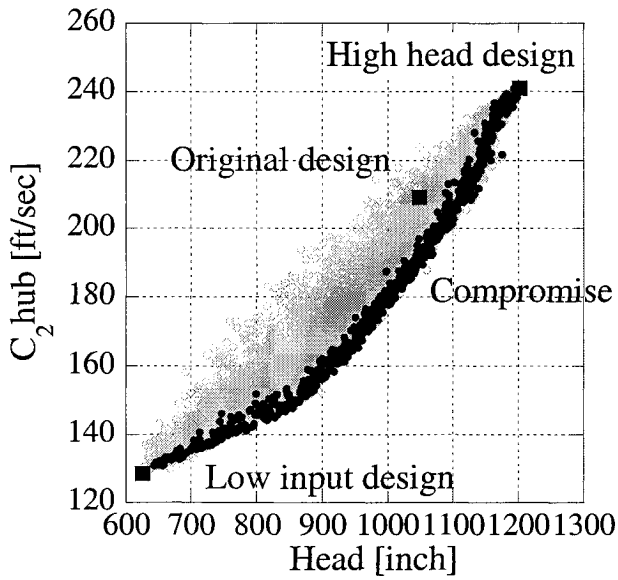

Figure 5. Flow velocity at second stage exit hub.

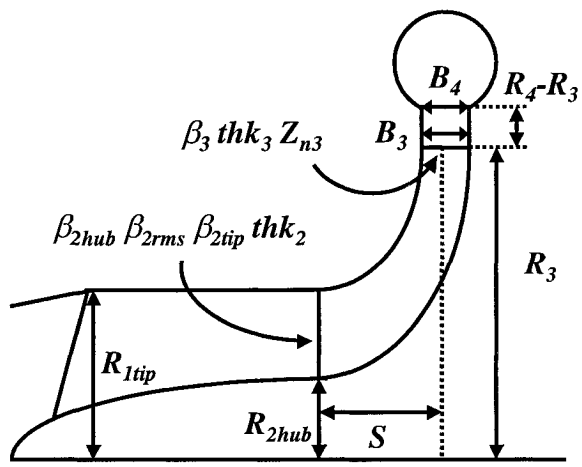

Figure 7. Design parameters of the multistage pump design problem.

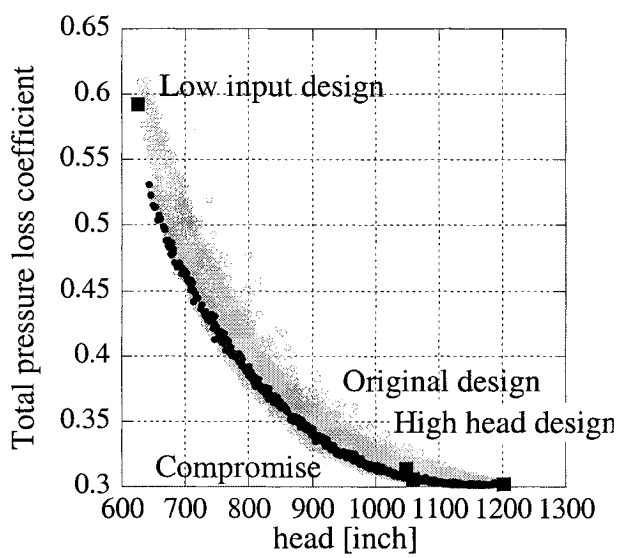

Figure 6. Total pressure loss coefficient of the centrifugal pump designs.

Table 3. Design parameter ranges of the multistage pump design problem.

<1st stage>

design variables	R_{tip} [inch]	R_{2hub} [inch]	β_{2hub} [degs.]	β_{2rms} [degs.]	β_{2tip} [degs.]	thk_2 [inch]
Upper boundary	*1.18*	*0.53*	*50.0*	*40.0*	*35.0*	*0.08*
Lower boundary	*1.08*	*0.43*	*35.0*	*25.0*	*20.0*	*0.03*

<2nd stage>

design variables	R_2 [inch]	(R_4-R_3) [inch]	B_2 [inch]	B_3 [inch]	thk_3 [inch]	S [inch]	Z_{n3}	β_3 [degs.]
Upper boundary	*2.20*	*0.15*	*0.35*	*0.50*	*0.08*	*1.00*	*16*	*90.0*
Lower boundary	*2.00*	*0.05*	*0.15*	*0.30*	*0.03*	*0.80*	*8*	*60.0*

(c)2001 American Institute of Aeronautics & Astronautics or Published with Permission of Author(s) and/or Author(s)' Sponsoring Organization.

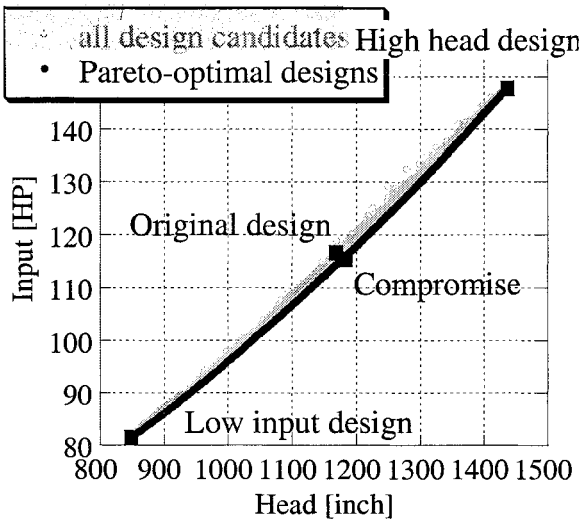

Figure 8. Objective function values of the multistage pump designs.

Table 4. Pareto-optimal designs of the multistage pump design problem.

<1st stage>

design variables	R_{tip} [inch]	R_{2hub} [inch]	β_{2hub} [degs.]	β_{2ms} [degs.]	β_{2tip} [degs.]	thk_2 [inch]
High head design	*1.17*	*0.517*	*49.9*	*38.5*	*34.9*	*0.0788*
Low input design	*1.17*	*0.525*	*42.9*	*37.3*	*28.0*	*0.0378*
Compromised design	*1.17*	*0.514*	*48.3*	*40.0*	*33.4*	*0.0520*
Original design	*1.13*	*0.480*	*43.0*	*27.3*	*21.6*	*0.0400*

<2nd stage>

design variables	R_3 [inch]	(R_4-R_3) [inch]	B_3 [inch]	B_4 [inch]	thk_3 [inch]	S [inch]	Z_{n3}	β_3 [degs.]
High head design	*2.20*	*0.1350*	*0.340*	*0.301*	*0.0311*	*0.855*	*16*	*87.4*
Low input design	*2.00*	*0.0548*	*0.152*	*0.393*	*0.0798*	*0.804*	*8*	*64.4*
Compromised design	*2.16*	*0.0608*	*0.333*	*0.370*	*0.0439*	*0.812*	*9*	*77.8*
Original design	*2.10*	*0.0950*	*0.251*	*0.400*	*0.0300*	*0.878*	*12*	*90.0*

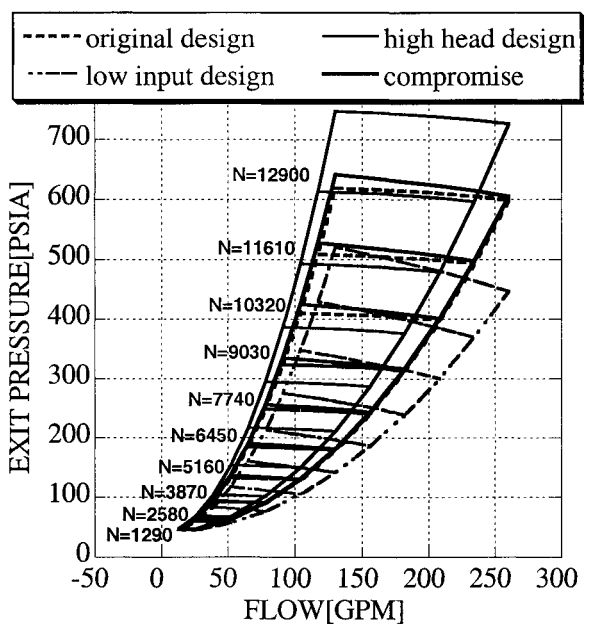

Figure 9. Pump overall performance map.

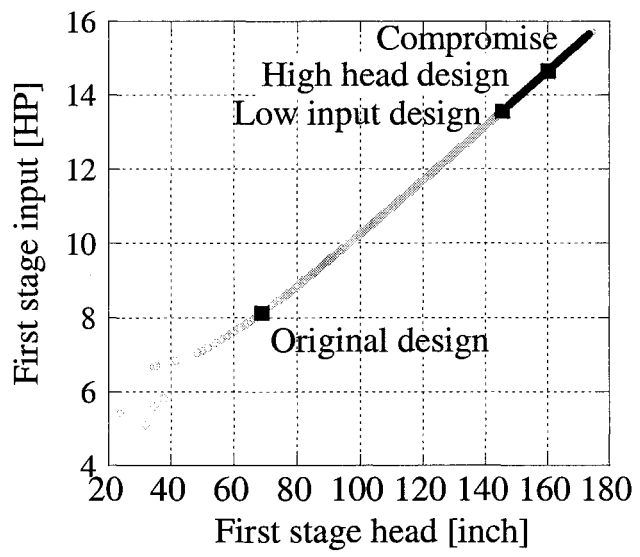

Figure 10. First stage performances of the multistage pump designs.

(c)2001 American Institute of Aeronautics & Astronautics or Published with Permission of Author(s) and/or Author(s)' Sponsoring Organization.

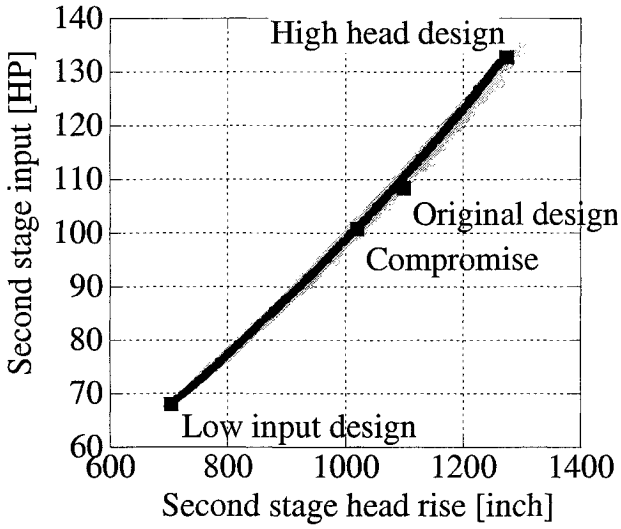

Figure 11. Second stage performances of the multistage pump designs.

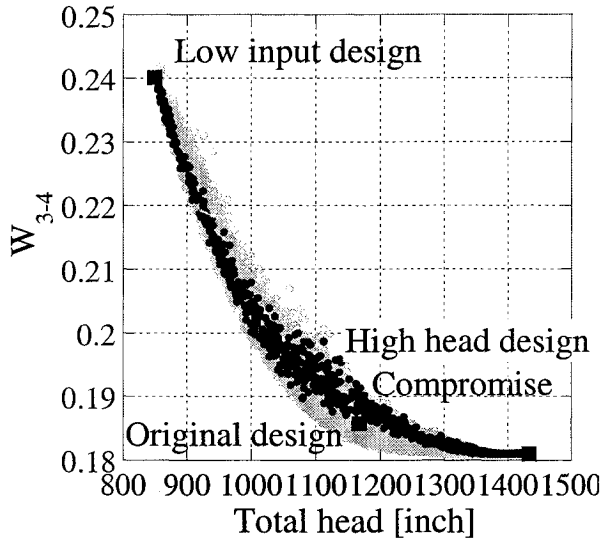
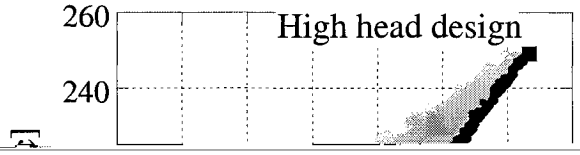
Figure 13. Total pressure loss coefficient of the multistage pump designs.